Article

Discovery of High-Affinity Ligands of Receptor, ERG2, and Emopamil Binding Protein by Pharmacophore Modeling and Virtual Screening

Christian Laggner, Claudia Schieferer, Birgit Fiechtner, Gloria Poles, Rmy D. Hoffmann, Hartmut Glossmann, Thierry Langer, and Fabian F. Moebius

J. Med. Chem., **2005**, 48 (15), 4754-4764• DOI: 10.1021/jm049073+ • Publication Date (Web): 24 June 2005

Articles

Discovery of High-Affinity Ligands of σ_1 Receptor, ERG2, and Emopamil Binding Protein by Pharmacophore Modeling and Virtual Screening

Christian Laggner,[†] Claudia Schieferer,[†] Birgit Fiechtner,[‡] Gloria Poles,[‡] Rémy D. Hoffmann,[§] Hartmut Glossmann,[‡] Thierry Langer,*[,†] and Fabian F. Moebius*[,‡]

Institute of Pharmacy, Department of Pharmaceutical Chemistry, and Center for Molecular Biosciences (CMBI), University of Innsbruck, Innrain 52, A-6020 Innsbruck, Austria; Department of Biochemical Pharmacology, Innsbruck Medical University, Peter-Mayr-Str. 1, A-6020 Innsbruck, Austria; and Accelrys SARL, Parc Club Orsay Université, 20, rue Jean Rostand, 91898 Orsay Cédéx, France

Received November 17, 2004

ERG2, emopamil binding protein (EBP), and sigma-1 receptor (σ_1) are enzymes of sterol metabolism and an enzyme-related protein, respectively, that share high affinity for various structurally diverse compounds. To discover novel high-affinity ligands, pharmacophore models were built with Catalyst based upon a series of 23 structurally diverse chemicals exhibiting K_i values from 10 pM to 100 μM for all three proteins. In virtual screening experiments, we retrieved drugs that were previously reported to bind to one or several of these proteins and also tested 11 new hits experimentally, of which three, among them raloxifene, had affinities for σ_1 or EBP of <60 nM. When used to search a database of 3525 biochemicals of intermediary metabolism, a slightly modified ERG2 pharmacophore model successfully retrieved 10 substrate candidates among the top 28 hits. Our results indicate that inhibitor-based pharmacophore models for σ_1, ERG2, and EBP can be used to screen drug and metabolite databases for chemically diverse compounds and putative endogenous ligands.

Introduction

Emopamil binding protein (EBP, vertebrate 3β-hydroxysteroid Δ^8-Δ^7 isomerase, EC 5.3.3.5) and its fungal counterpart ERG2 (EC 5.3.3.5, e.g. from *Saccharomyces cerevisiae*) are 25−27 kDa integral membrane proteins of the endoplasmic reticulum. Both bind a variety of chemicals from different pharmacological classes with nanomolar affinity.[1] EBP and ERG2 catalyze the shift of a double bond in the B-ring of the sterol nucleus from C_{8-9} to C_{7-8} and require no cofactors. The sigma$_1$ receptor (σ_1; official gene designation in the Human Gene Nomenclature Database: opioid receptor sigma 1, OPRS1) is a gene product of vertebrates that is highly homologous with ERG2 from yeast but lacks 3β-hydroxysteroid Δ^8-Δ^7 isomerase activity.[2] The σ_1 receptor has been reported to mediate a plethora of pharmacological effects but is functionally and structurally unrelated to other opioid receptors (reviewed by Moebius et al.[3] and Bowen[4]). While the amino acid sequences of the σ_1 receptor and ERG2 are 30% identical, EBP is structurally unrelated with σ_1 and ERG2, despite similar molecular masses. Hydropathy plots of the amino acid sequences suggested that the σ_1 receptor and ERG2 have three putative transmembrane domains, while EBP has four.[3]

We previously reported striking similarities of the pharmacological profiles of EBP and ERG2 on one hand, and structural similarities between ERG2 and the σ_1 receptor on the other hand.[1,5] Therefore, the aim of our current study was to use pharmacophore modeling (i) to create a rational basis for the similarity of the pharmacological profiles, (ii) to search in silico for novel high affinity ligands, (iii) to create virtual counterscreen filters to remove high-affinity ligands of the σ_1 receptor and EBP from drug databases, (iv) to predict the affinity of high-energy reaction intermediates for both enzymes with pharmacophore models, and (v) to test whether pharmacophore models based on affinities for enzyme inhibitors could be used to identify endogenous receptor ligands and substrates from metabolite databases. Several molecular modeling studies have been performed for the σ_1 receptor.[6−9] However, none of these could be applied to database screening for the retrieval of new hit compounds. To the best of our knowledge, no computational models have yet been reported for ERG2 and EBP.

Methods

Generation of Pharmacophore Models. Pharmacophore models were generated for all three targets with the HypoGen module of Catalyst using all the compounds from the training set with their corresponding affinity data (Table 1), with the exception of the EBP model, where compound **12** was left out to yield hypotheses with higher correlations. All possible combinations of the following feature types, with a maximum of five features per hypothesis, were allowed: (i) H-bond acceptors, (ii) H-bond donors, (iii) hydrophobic, (iv) positive

* To whom correspondence should be addressed. T.L.: phone, +43-512-5075252; fax, +43-1-8174955-1371; e-mail, thierry.langer@uibk.ac.at. F.M.: phone, +43-512-5073168; fax, +43-512-507-2858; e-mail, fabian.moebius@uibk.ac.at.
[†] University of Innsbruck.
[‡] Innsbruck Medical University.
[§] Accelrys SARL.

10.1021/jm049073+ CCC: $30.25
Published on Web 06/24/2005

Table 1. The Training Set

	K_i EBP (nM)		K_i σ_1 (nM)		K_i ERG2 (nM)	
compd	measured	estimated	measured	estimated	measured	estimated
1	2200[13]	1300	6[2]	15	1200[14]	400
2	25[13]	7.8	1[5]	0.45	62[14]	1.5
3	4[1]	7.4	0.5[5]	0.12	65	2.2
4	>100000	140000	35600[2]	1400	>100000[14]	25000
5	6700[13]	810	15[2]	10	2000[14]	260
6	6[13]	7.1	1[2]	1.6	65[14]	360
7	18[13]	43	4[2]	9	74[14]	360
8	1[1]	0.49	8[5]	17	160[5]	460
9	30[1]	9.3	0.01[5]	0.005	0.05[14]	0.044
10	190[13]	1200	0.2[2]	0.74	0.5[14]	6.4
11	5[1]	22	2[2]	4.3	1[14]	3.2
12	1[1]	100	0.6[5]	1.2	5[5]	13
13	0.6[1]	2.5	0.5[5]	0.5	0.4[5]	1.9
14	13[13]	58	0.2[2]	3	17[14]	60
15	500[13]	1300	1.7[2]	9.5	1000[14]	780
16	>100000	190000	260[2]	660	4430[14]	6700
17	9300[13]	1400	40[2]	11	4700[14]	450
18	5[1]	5.3	35[5]	13	1500	270
19	>100000	140000	1200[2]	1400	7760[14]	25000
20	1[1]	2.6	0.04[5]	0.027	0.09[14]	0.11
21	8[13]	8.5	15[2]	7.7	500[14]	280
22	11[1]	6.5	8[5]	3	2[14]	2.6
23	2[1]	2.3	5[5]	3.3	2[5]	10

Table 2. Statistical Values for Pharmacophore Models Generated with Catalyst

hypothesis	total cost	Δ cost	rmsd	correlation
EBP	104.72	128.55	1.026	0.965
σ_1	104.78	71.86	1.113	0.926
ERG2	118.21	113.29	1.461	0.918

ionizable, and (v) aromatic ring. For each target (σ_1, EBP, ERG2), 10 hypotheses were reported, from which the ones with the highest correlation values were chosen as our pharmacophore models.

Assessment of the Quality of Pharmacophore Hypotheses. To assess the statistical relevance of our three models we performed the following tests.

Cost Analysis. The cost value of a pharmacophore hypothesis and especially its difference to the cost of the null hypothesis is an important indicator for the statistical relevance of the hypothesis. According to the Catalyst documentation, a high probability for the models to represent a true correlation is given if the difference between these two values is larger than 70, which is the case for all three of our reported models (Table 2).

Randomization Test. Using the module CatScrambe, the molecular spreadsheets of our three training sets were modified by arbitrary scrambling of the affinity data for all compounds. These randomized spreadsheets should yield hypotheses without statistical significance; otherwise, the original model is also random. To achieve a statistical significance level of 95%, 19 random spreadsheets were generated for each of our three hypotheses. For all three targets, randomization tests gave hypotheses with total cost values lying well above those reported for the sets of original hypotheses, yielding lower values for the differences $\text{cost}_{\text{null-hypothesis}} - \text{cost}_{\text{total}}$, further supporting the statistical significance of our models. A detailed discussion of cost analysis is given by Krovat and Langer.[10]

Automatic Affinity Prediction. Automatic affinity prediction of the compounds did not always lead to reasonable alignments, since some compounds with many flexible lipophilic residues were aligned in a way in which all hydrophobic spheres fitted perfectly, while the supposedly substantial basic amino group did not fit the positive ionizable feature. Nevertheless, manual alignment via tethers between the amino group and the positive ionizable feature usually lowered the predicted affinity values by less than 3-fold. Therefore, only the values retrieved from automatic alignments are given in Table 3.

Database Searches. Our pharmacophore models were used to search the Thomson Derwent World Drug Index (WDI, version 960612, 48 405 molecules), a database of marketed and developmental drugs, to validate the models by finding both known and novel ligands for our target proteins. Furthermore, we searched a 3525 metabolite subset of the KEGG (Kyoto Encyclopedia of Genes and Genomes) COMPOUND database, which comprises endogenous metabolites as well as products of xenobiotic metabolism.[11,12]

Results

Structurally Diverse Training Sets Covering a Broad Range of Affinities. The training sets were chosen to represent structurally diverse compounds for which the affinity had been determined under identical

Table 3. Measured and Estimated Affinities for the Test Set

	K_i EBP (nM)		K_i σ_1 (nM)		K_i ERG2 (nM)	
compd	measured	estimated	measured	estimated	measured	estimated
24	34000[1]	6.7	680[1]	0.36	16480[1]	6.5
25	54[1]	3	3[1]	0.49	0.7[1]	0.11
26	0.9[1]	2.9	30[1]	6.1	232[1]	220
27	1500[1]	1600	880[1]	9	310	960
28	2	45	1[3]	0.27	13	1.8
29	3	2.3	3	0.41	9	3.1
30	>50000[1]	230	ND[a]	8.7	>50000[1]	140
31	165[1]	430	0.83[5]	0.44	0.15[14]	13
32	2[1]	26	1[1]	3.4	0.2[1]	4.4

[a] ND: not determined.

Chart 1. Structures of Molecules in the Training Set[a,b]

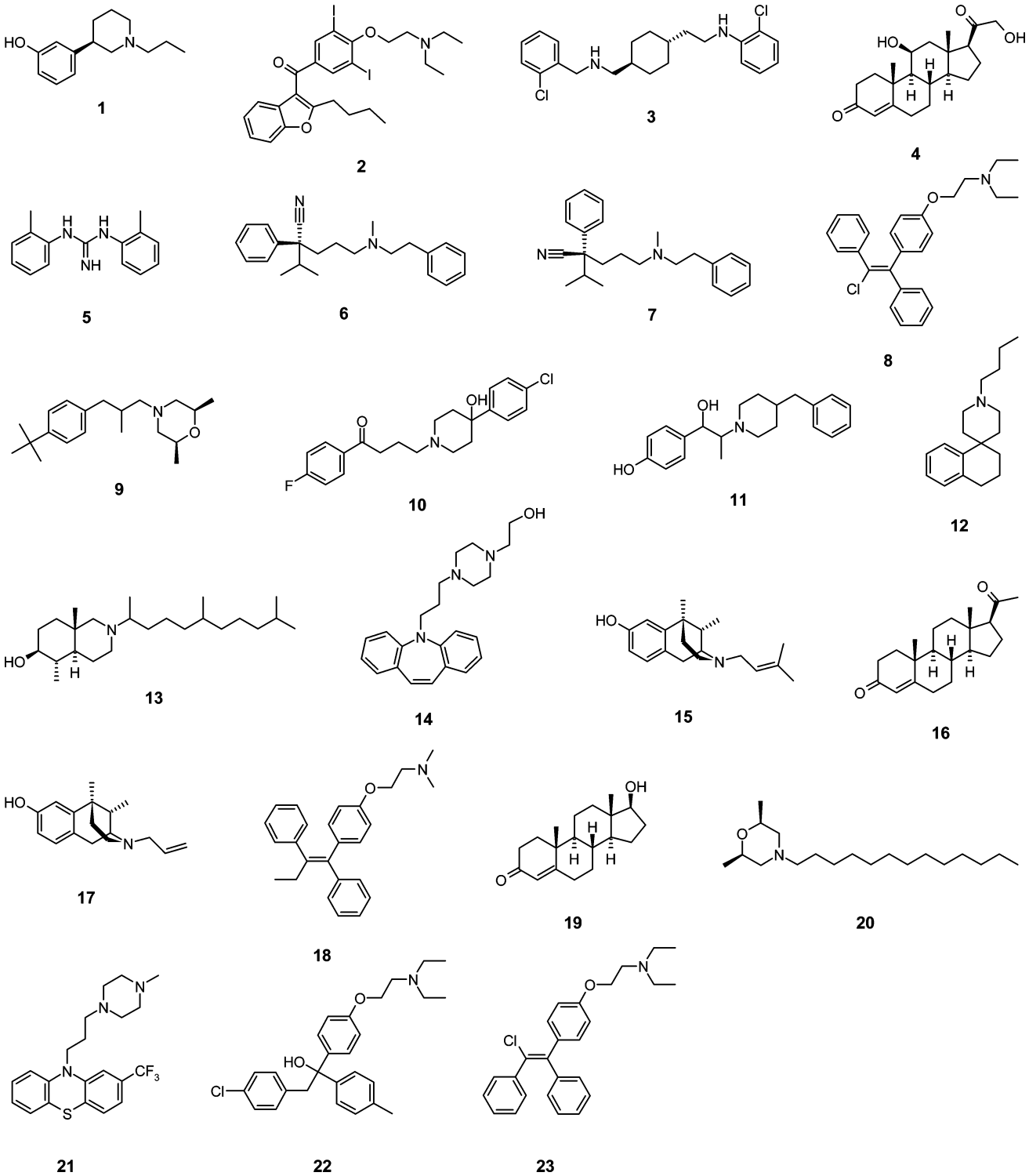

[a] **1**, (+)-3-PPP; **2**, amiodarone; **3**, AY-9944; **4**, corticosterone; **5**, 1,3-di-o-tolylguanidine; **6**, (+)-emopamil; **7**, (−)-emopamil; **8**, enclomiphene; **9**, fenpropimorph; **10**, haloperidol; **11**, ifenprodil; **12**, L-690,404; **13**, MDL-28,815; **14**, opipramol; **15**, (+)-pentazocine; **16**, progesterone; **17**, (+)-SKF-10,047; **18**, tamoxifen; **19**, testosterone; **20**, tridemorph; **21**, trifluoperazine; **22**, triparanol; **23**, zuclomiphene [b] Where chiral stereocenters are undefined (**9**, **11**, **13**, and **22**), compounds were tested as mixtures of stereoisomers.

experimental conditions for all three proteins.[1,5] Drugs were selected from different pharmacological classes, such as antidepressants (opipramol, **14**), nuclear hormone receptor ligands (tamoxifen, **18**; zuclomiphene, **23**; enclomiphene, **8**), antipsychotics (trifluperidol, **31**; haloperidol, **10**; trifluoperazine, **21**), calcium antagonists (emopamil, **6** and **7**; amiodarone, **2**), fungicides (fenpropimorph, **9**; tridemorph, **20**), opioid analgesics ((+)-pentazocine, **15**; (+)-SKF-10,047, **17**), σ ligands ((+)-3-PPP, **1**; ditolylguanidine, **5**), sterol biosynthesis inhibitors (triparanol, **22**; AY-9944, **3**; MDL-28,815, **13**), and steroids (corticosterone, **4**; progesterone, **16**; testosterone, **19**) (Chart 1). The K_i values covered a range from 0.6 nM to 100 μM for EBP, 10 pM to 36 μM for σ_1 receptor, and 50 pM to 100 μM for ERG2; 58%, 54%, and 38% of the 23 compounds were in the range of

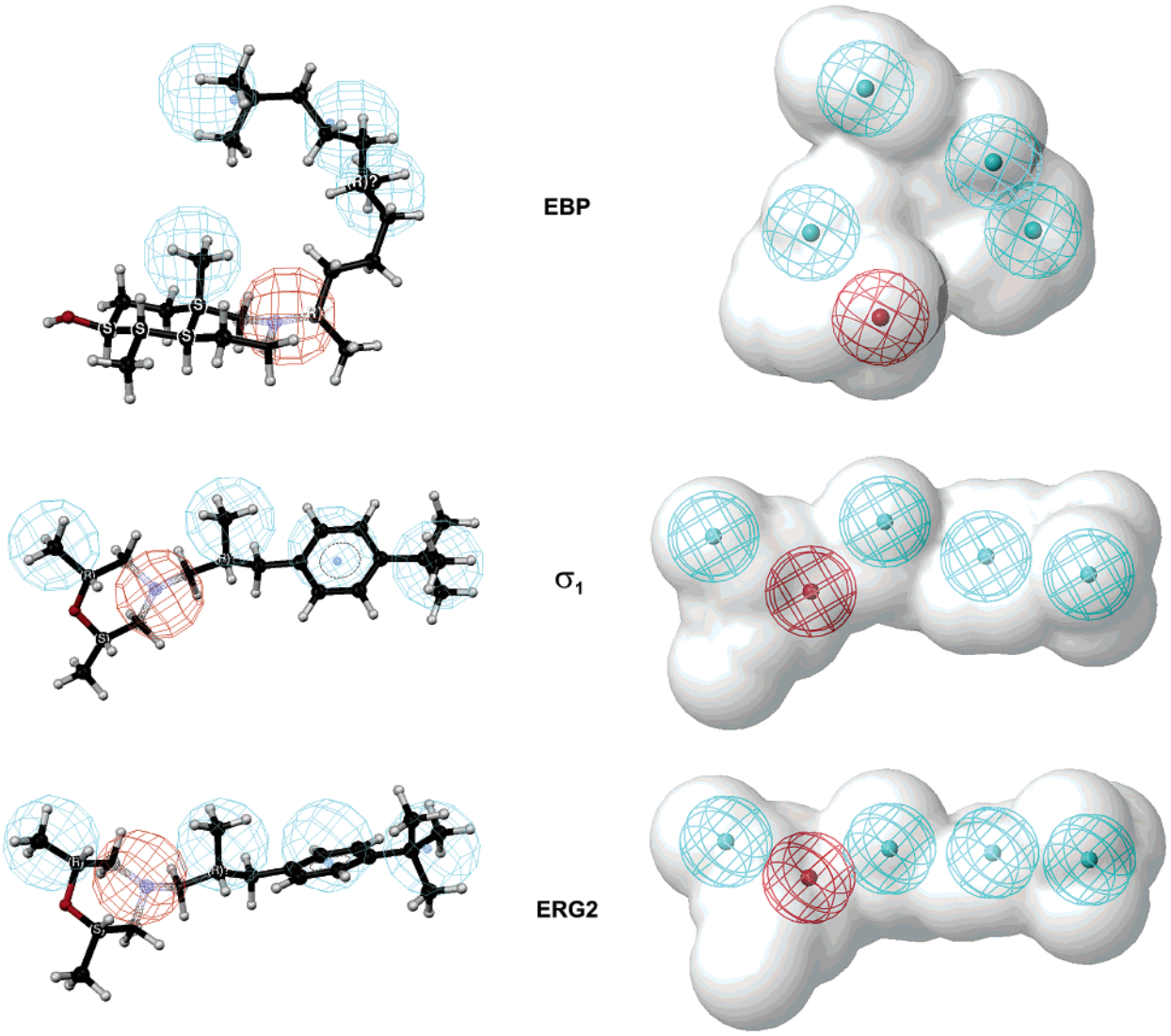

Figure 1. (Left panel) Pharmacophore models for EBP, σ_1, and ERG2 mapped by high-affinity ligands **13** (EBP) and **9** (σ_1 and ERG2): cyan spheres, hydrophobic features; red spheres, positive ionizable feature. (Right panel) Hypotheses with added shape volumes of high-affinity ligands **8** (EBP) and **9** (σ_1, ERG2) which were used for searching the WDI database.

1−100 nM for EBP, σ_1 receptor, and ERG2, respectively (Table 1). The selectivity of compounds varied with six chemicals differing less than 10-fold, 13 chemicals less than 100-fold, and all but one less than 1000-fold in their affinity for EBP, σ_1 receptor, and ERG2.

All Three Models Have One Positive Ionizable and Four Hydrophobic Features in Common. For all three proteins, the best scoring models consisted of four hydrophobic features and one positive ionizable feature. The left panel of Figure 1 shows these models, together with their most active ligands. All three models are surprisingly simple and require only two of the available feature types, i.e., positive ionizable and hydrophobic, but no directed hydrogen bonds or aromatic rings. The predicted and experimentally measured K_i values of the training set were in excellent agreement (correlation coefficients of 0.93, 0.92, and 0.97 for σ_1, ERG2, and EBP, respectively, Table 2). The right panel of Figure 1 shows the same models with the added shape volumes of the van der Waals radii. We calculated the volumes and surfaces of the van der Waals radii of the five ligands with the highest affinity for each of the three proteins within Sybyl 6.91[15] that revealed no significant differences [σ_1 (**3**, **9**, **13**, **14**, **20**), volume = 401 ± 33 Å^3, surface 284 ± 24 Å^2; EBP (**3**, **8**, **13**, **20**, **23**), 419 ± 22 Å^3, surface 300 ± 19 Å^2; ERG2 (**9**, **10**, **11**, **13**, **20**), 387 ± 36 Å^3, surface 274 ± 24 Å^2]. Our pharmacophore model for the σ_1 receptor is in good agreement with the model reported by Glennon et al.,[16] who suggested a basic amino nitrogen atom between two hydrophobic sites. The primary hydrophobic site of Glennon's model, which is at an optimum distance of 7−9 Å from the amino group, corresponds with our two distal hydrophobic feature spheres, which are mapped by the *tert*-butyl and phenyl moieties of **9** (6.3 and 9.8 Å from the amino group), while the secondary hydrophobic site is matched by the sphere that maps to the methyl group attached to the morpholine ring (reported distance 2.5−3.9 Å from the amino group, in our model 4.1 Å) (Figure 1). Coordinates and distance matrixes for all features of each HypoGen model are given as Supporting Information.

The Pharmacophore Models Are Sound and Predict Well within the Scope of Their Application for Virtual Screening. Compounds in the test set were chosen arbitrarily, covered a broad range of affinities from 0.2 nM to 34 μM, and represented different pharmacological classes, such as inhibitors of

Chart 2. Structures of Molecules in the Test Set[a,b]

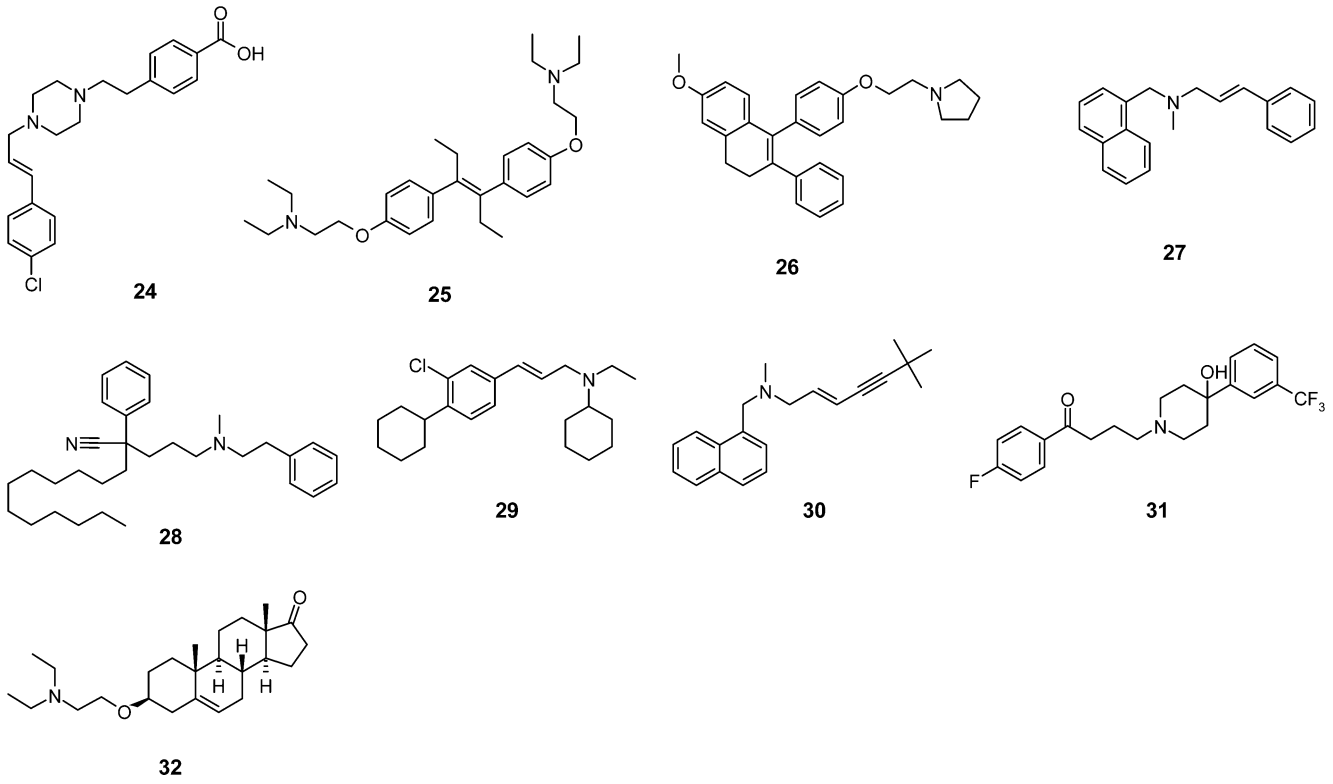

[a] **24**, BM-15766; **25**, MDL-5332; **26**, nafoxidine; **27**, naftifine; **28**, ronipamil; **29**, SR-31747; **30**, terbinafine; **31**, trifluperidol; **32**, U-18666A. [b] Compound **28** was tested as a racemic mixture.

cholesterol biosynthesis (SR-31747, **29**; U-18666A, **32**; BM-15766, **24**), antipsychotics (trifluperidol, **31**), antimycotics (naftifine, **27**; terbinafine, **30**), calcium antagonists (ronipamil, **28**), and estrogen receptor modulators (MDL-5332, **25**; nafoxidine, **26**) (Chart 2).

For each of the three proteins, spreadsheets containing the test set compounds were generated, and the affinities were predicted with the three different pharmacophore models and compared with experimental data (Table 3).

From 26 measured affinities, 14 were predicted correctly within 1 order of magnitude. Among those values where the results differed by more than 1 order of magnitude, false-positive results (i.e. overestimation of affinity) occurred 10 times, while false-negative results (i.e. underestimation of affinity) were retrieved only in two cases. We therefore considered that overestimation of affinity might originate from the propensity of Catalyst to predict high affinities as long as the compounds map all or most of the pharmacophore features without consideration of sterical hindrance, for example, by bulky ligand side chains. In reality, these compounds, even though they have all five required pharmacophore features, may not fit into the actual binding site. In an attempt to refine our models, we used Catalyst's HypoRefine module, which generates pharmacophore models possessing a variable number of so-called excluded volume spheres, i.e., "forbidden zones", that must not be mapped by the fitted compound. Information for the location of the excluded volume spheres is mostly drawn from inactive compounds. However, the models produced by HypoRefine did not contain any excluded volume spheres and were very similar to those produced by HypoGen (data not shown), presumably because in our training set the low-affinity compounds were primarily the nonbasic, sterically rather undemanding steroid compounds **4**, **16**, and **19**. Moreover, while the inclusion of such compounds in the training set whose low affinity is due to sterical demands may lead to valuable improvements in models that are less linear and where compounds are fixed, for example, by hydrogen bonds, they would be of little use for our models, especially those for ERG2 and for the σ_1 receptor, which provide various possibilities for the compounds to match. Thus, it is very likely that inclusion of a few excluded volume spheres would still not prevent these compounds from matching. The fact that the measured affinities for compound **24** are considerably lower than the predicted values may also be attributable to the amphotheric character of this compound, which is the only one of our investigated compounds that bears a carboxylic acid group.

Hydrogen Bond Interactions Are Not Required for High-Affinity Inhibitor Binding. For sterols as EBP isomerization substrates, the importance of a 3β-hydroxy group has been demonstrated.[17] Some of the basic ligands in the training set (**1**, **11**, **13**, **14**, **15**, **17**) bear hydroxy groups that indeed are as distant from the basic amino group as the 3-hydroxy group is from the positively charged C_8 of the carbocationic sterol substrates. However, this putative additional hydrogen bond does not seem important for ligands of σ_1, EBP, and ERG2, since our training and test sets contained many high-affinity ligands devoid of these hydrogen bonds (e.g. **6**, **9**, **12**, **20**) which were estimated as well as hydroxy-bearing compounds. In addition, the fact that the σ_1 affinities of 2′-deoxy analogues of pentazocine, SKF-10,047, and related benzomorphanes were

Table 4. Successive Reduction of the Hit Lists Received from Searching the WDI Database[a]

	no. of compd hits and % of total database		
hypothesis	with original hypothesis	+ MW ≤ 600 and $K_{i\,est}$ ≤ 100 μM	+ shape filtering
EBP	4165 (8.60)	771 (1.59)	670 (1.38)
s1	2768 (5.72)	1582 (3.27)	389 (0.80)
ERG2	2605 (5.38)	1022 (2.11)	303 (0.63)

[a] Hits are compounds that map all five pharmacophore features.

very similar to those of their parental structures[18] further supports our conclusion that hydrogen-bond interactions are not important for inhibitor binding.

Similarity of σ_1 and ERG2 but Not EBP Pharmacophore Models. Superposition of the two models for the structurally related proteins σ_1 and ERG2 displayed their striking similarity (not shown), which is in line with the high correlation of the K_i values between the compounds in the training sets for both proteins [correlation coefficients for pK_i(ERG2) vs pK_i(σ_1) = 0.83; pK_i(EBP) vs pK_i(ERG2) = 0.58]. Because of the aforementioned similarity of the σ_1 and ERG2 models, we compared these two to the EBP model. Despite the identical biochemical function of EBP and ERG2, which is 3β-hydroxysteroid Δ^8-Δ^7 isomerization, and also despite the same number and type of features for all three models, the location of features differed substantially between EBP and σ_1/ERG2. The features for the EBP hypothesis did not assume the almost linear alignment of the other two models, but rather formed a five-cornered, almost planar structure. The EBP pharmacophore can bind bulky compounds such as **8**, **18**, and **26** with high affinity, whereas linear compounds such as **9**, **10**, **20**, and **31** tend to show higher affinity for σ_1 and ERG2 than for EBP.

Efficient Discovery of New Ligands in a Three-Dimensional Drug Database. The search for new ligands within the WDI database produced 2605−4165 initial hits for the three different targets (Table 4). These initial hits were filtered for compounds with a predicted K_i value < 100 μM and a molecular weight < 600. Further filtering with the molecular shape of the high affinity ligand **8** for EBP and **9** for σ_1 and ERG2 gave 0.6−1.4% hits for each protein (Table 4; Figure 1, right panel), which is in the same range as for other pharmacophore models.[10,19−21]

As expected, the database search retrieved compounds that had been part of our training and test sets (**3**, **8**, **9**, **13**, **20**, **22**, **23**, and **32**), but also many others, among them the fungicide amorolfine **37**, which is closely related to **9** and **20**, and several ligands with known K_i values for σ_1 (**38**, 5 nM;[22] **39**, 16 nM;[23] **40**, 1.0 nM;[24] **41**, 8554 nM;[25] **42**, 2.5 nM[26]) and for EBP (**40**, 15 nM[24]) (Chart 3). Additionally, we found 22 compounds that incorporate steroidal substructures and a basic amino residue, of which 19 were identified as steroidal alkaloids. These natural products are derivatives of cholesterol isolated from plants, which often incorporate additional ring systems or show modified ring sizes.

After visual inspection of the hits identified in the WDI, requests for samples were sent out for 23 of those hits that were of synthetic origin and showed predicted K_i values smaller than 100 nM for at least one target. Of these, four were eventually obtained and experimentally tested together with two commercially available substances (Chart 3, Table 5). Among these compounds were buflomedil (**43**, α_1-adrenoceptor blocker), CP-74932-4 (**44**, experimental antibiotic), carbisocaine (**45**, local anesthetic), R-59494 (**46**, experimental calcium antagonist), and raloxifene (**47**, partial estrogen receptor agonist), as well as compound VUF-8410 (**48**), closely related to hit VUF-8405 (**49**, experimental antihistaminergic, no longer available). Furthermore, the following five steroidal alkaloids were also selected and experimentally tested: tomatidine (**50**, from tomatos), solasodine (**51**, from *Solanum* species), solanidine (**52**, from potatos), cyclopamine, and jervine (**53** and **54**, from *Veratrum californicum*) (Chart 3, Table 5).

Table 5. Measured Affinities for Compounds Identified in the WDI Database

	K_i (nM)		
	EBP	σ_1	ERG2
43	60	1290	7150
44	8500	26700	31700
45	51	230	2800
46	450	1.3	169
47	1	38	66
48	39	6	170
50	583	81	387
51	>100000	207	1170
52	441	74	>100000
53	654	>100000	500
54	>100000	>100000	284

Of the synthetic compounds, **43** and **47** possessed good selectivity for EBP, while **46** possessed excellent selectivity for σ_1. Except for compound **44**, which incorporates a rather atypical *N*-(2-thiazolyl)guanidine moiety and which showed only weak affinities for all three proteins, each of the tested synthetic compounds interacted at least with one protein with a K_i value ≤60 nM. The efficiency of our search was excellent, retrieving three and four lead compounds out of six tested with K_i values ≤60 nM for σ_1 and EBP, respectively (Table 5). All of the five tested steroidal alkaloids showed K_i values ≤500 nM for at least one target, with two compounds (**50** and **52**) showing K_i values <100 nM for the σ_1 receptor (Table 5). Cyclopamine (**53**) and jervine (**54**) have been shown to exhibit teratogenicity and to be potent inhibitors of the Sonic hedgehog pathway[27] by inhibiting the multipass transmembrane protein smoothened.[28] It is noteworthy that these two compounds did not show any affinity for the σ_1 receptor, while on the other hand tomatidine (**50**), which is not teratogenic and acts as a negative comparison compound in hedgehog inhibition tests, shows good affinity for σ_1 (K_i = 81 nM), revealing complementary selectivity of **50** on one side and of **53** and **54** on the other side for these two different targets. These natural compounds differ from most of the synthetic ligands by the absence of a phenyl moiety and (in four out of five cases) by the occurrence of a secondary amine. Furthermore, they show very little flexibility, which makes them interesting candidates for evaluating the sterical limits of the binding pockets. We assume that, compared to the natural steroid substrates, **50**−**54** fit the binding pockets in a reversed way; i.e., in our models, the A ring of the steroidal alkaloids matches that hydrophobic feature that is farthest away from the positive ionizable feature.

Chart 3. Compounds That Were Retrieved by Searching the WDI Database, with either Known Affinity for EBP and σ_1 (**37**−**42**) or Compounds Newly Tested for Their Affinities at These Targets, Being of Both Synthetic (**43**−**48**) and Natural (**50**−**54**) Origin[a,b]

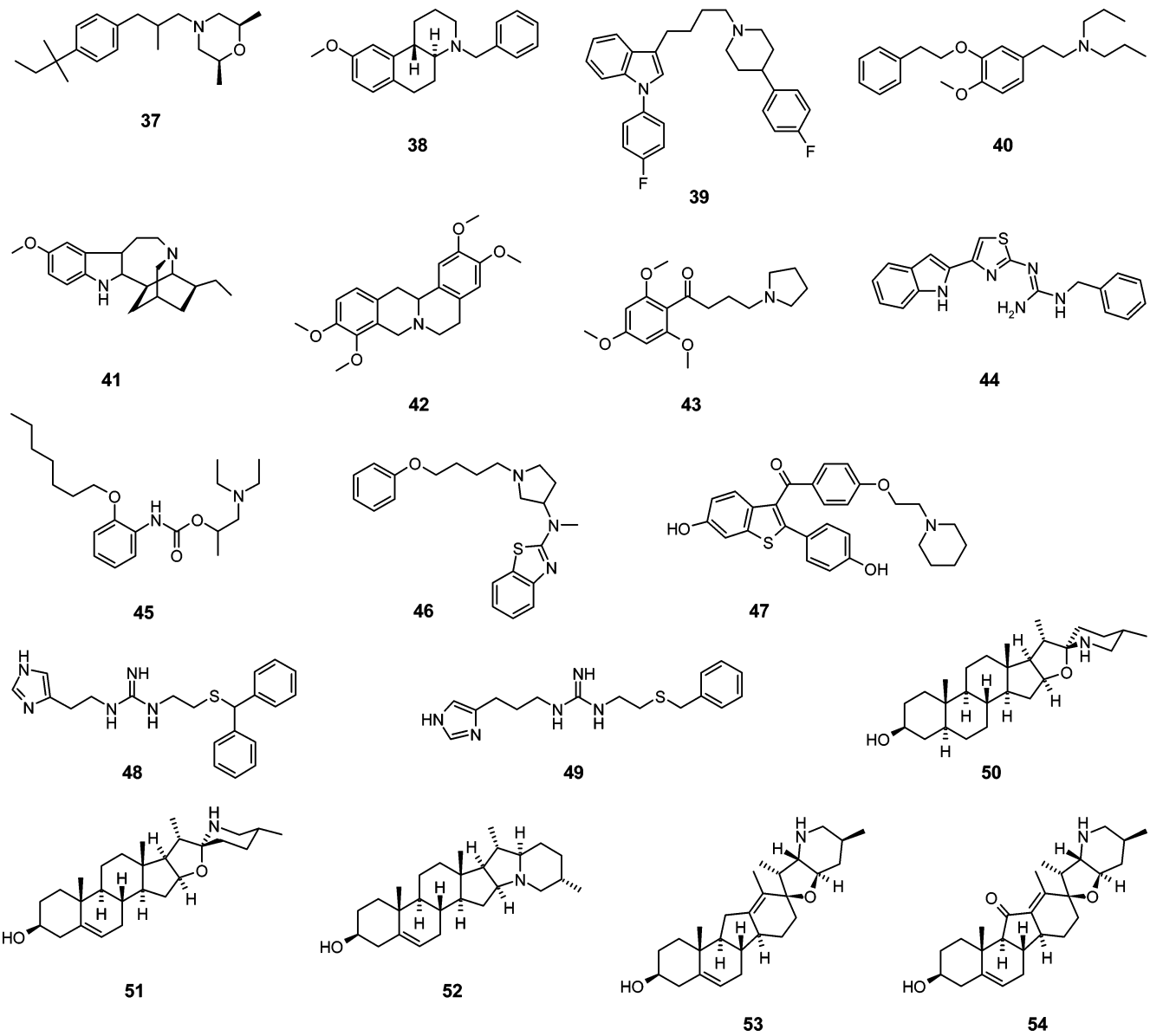

[a] **37**, amorolfine; **38**, HW-173; **39**, LU 29,253; **40**, NE-100; **41**, ibogaine; **42** tetrahydropalmatine; **43**, buflomedil; **44**, CP-74932-4; **45**, carbisocaine; **46**, R-59494; **47**, raloxifene; **48**, VUF-8410; tested in place of **49**, VUF-8405; **50**, tomatidine; **51**, solasodine; **52**, solanidine; **53**, cyclopamine; **54**, jervine. [b] Compounds **45** and **46** were tested as racemic mixtures.

Nanomolar Affinity Predicted for Reaction Intermediates of 3β-Hydroxysteroid Δ^8-Δ^7 Isomerization. Both 3β-hydroxysteroid Δ^8-Δ^7 isomerases, EBP and ERG2, trigger the isomerization reaction by protonation of their sterol substrates at C_9, followed by formation of the high-energy intermediates (HEI) positively charged at C_8 and subsequent elimination of a proton at C_7 (Scheme 1).

According to isotopic labeling experiments, in EBP the hydrogen is eliminated at the 7β position via a trans hydrogen addition−elimination reaction, while in ERG2 a cis addition−elimination reaction results in the loss of the 7α hydrogen.[29] Since the proposed HEI is short-lived, it is not possible to directly measure the affinity of the HEI for EBP and ERG2. Instead, we predicted the virtual K_d value for the HEI with our pharmacophore models for ERG2 and EBP, respectively. It is noteworthy that these models are based on enzyme inhibitor rather than on substrate affinities. The HEIs were constructed from the two substrates of EBP and ERG2, zymosterol (**33**) and fecosterol (**34**), respectively. Figure 2 illustrates that especially the HEI of ERG2 aligns well with the pharmacophore model and that both carbocations are indeed high-affinity ligands (**33**, estimated $K_{d(HEI)}$ for EBP = 89 nM and ERG2 = 1.5 nM; **34**, estimated $K_{d(HEI)}$ for EBP = 1600 nM and ERG2 = 0.07 nM).

Virtual Substrate Retrieval from the KEGG Metabolite Database. Since our EBP and ERG2 models recognized the HEI of their substrates as high-affinity ligands, we investigated whether the pharmacophore models were able to selectively retrieve potential substrates that possess a double bond either at C_7−C_8 or—because of the reversibility of the reaction—at C_8−C_9, from the KEGG database of biochemicals of intermediary metabolism (metabolites). Such a metabo-

Scheme 1. Isomerization Reaction of Zymosterol (**33**) and Fecosterol (**34**) to 3β,5α-Cholesta-7,24-dien-3-ol (**35**) and 3β,5α-Ergosta-7,24(28)-dien-3-ol (**36**) by EBP and ERG2, Respectively

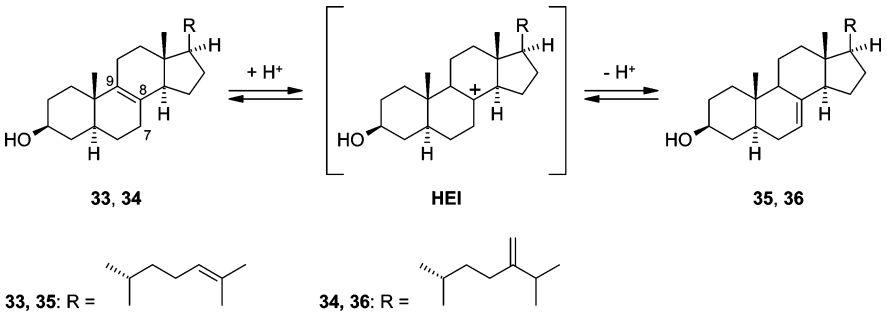

lite database search required that the pharmacophore models were able to find also nonbasic, isomerizable steroid substrates in their unprotonated form without building the carbocationic HEI. We therefore modified the positive ionizable feature of the original ERG2 pharmacophore model to also match carbon atoms that are part of a C=C double bond. The differences between conformational models for protonated versus nonprotonated substrates were negligible with the only difference at C_9, which changed from a planar to a tetraedric configuration (data not shown). With the modified ERG2 pharmacophore model we first searched a small subset of the KEGG database containing 198 gonans. Out of these, 27 theoretically qualified as substrates because they carried a double bond at C_7−C_8 or C_8−C_9 and had high lipophilicity, i.e., less than five hydroxy or keto groups. It should be pointed out, however, that only nine of these fulfill substrate requirements because the remaining compounds have additional features, e.g. methylation at C_4 or C_{14}, that prevent catalysis[17,30] but are not considered by the pharmacophore model. Since the substrates in the database were in the unprotonated ground state that binds with low affinity (e.g. K_m of zymosterol for EBP = 25 μM[1]), we forewent the prediction of affinity constants. Instead we used Catalyst's fit values that range from 0 (meaning that the molecule does not fit the model) to the number of features in the pharmacophore model (in this case 5, which describes a perfect fit). With the FAST search method, the ERG2 pharmacophore model retrieved all 27 theoretical substrates showing fit values ≥3.00 ranked among the best 34 hits from the 198 gonans. Similar results were obtained for EBP (data not shown). These results indicated that the sensitivity of both models for finding putative HEIs among sterols with double bond at C_7−C_8 or C_8−C_9 was 100%. We next tested whether the modified pharmacophore models could retrieve putative substrates even from a comprehensive database (3525 compounds) of metabolites taken from the KEGG database. However, with the modified ERG2 pharmacophore model, hits were contaminated with false positives to a large extent. To improve retrieval of 3β-hydroxysteroids, we further modified the ERG2 pharmacophore model by introducing a nondirected hydrogen-bond donor feature at the position of the 3β-hydroxy group of the sterols as a sixth feature of the pharmacophore model. Although this feature is not required for enzyme inhibitor binding (see above), it is indispensable for catalytic activity.[17] This further modified ERG2 pharmacophore model successfully retrieved 28 metabolites as putative substrates with fit values >4.00 (theoretical maximum value 6.00). Among these metabolites were 10 sterols comprising the three actual substrates fecosterol (**34**, fit value = 4.52), zymosterol (**33**, fit value = 4.48), and zymostenol (**60**, fit value = 4.10), while most of the others were intermediates of sterol biosynthesis methylated at C_4 (**55**−**59**, **61**, **62**; Table 6).

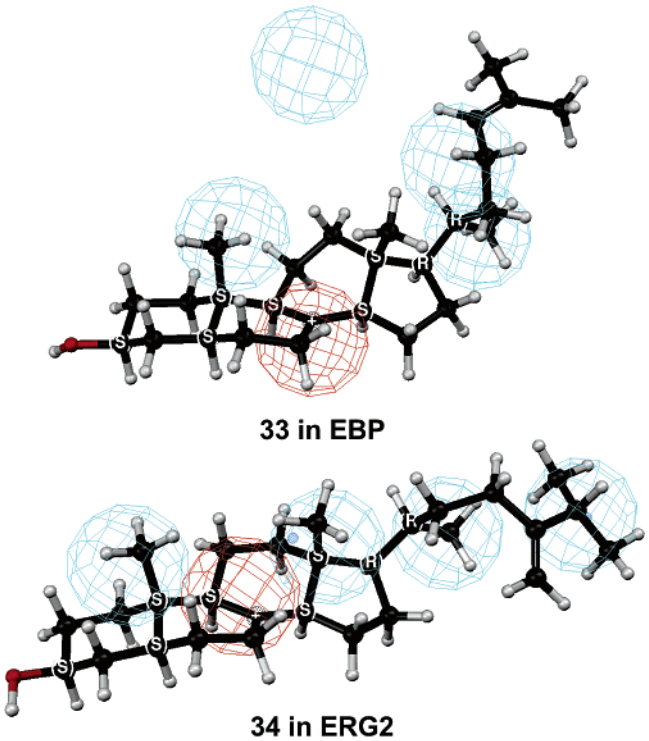

Figure 2. Proposed reaction intermediates obtained by protonation of zymosterol (**33**) and fecosterol (**34**) mapped to the pharmacophore models for EBP and ERG2: cyan spheres, hydrophobic features; red spheres, positive ionizable feature.

Among the other metabolites with fit values >4.00 were sterol-derived vitamins [ergocalciferol (vitamin D_2), fit value = 4.68; cholecalciferol (vitamin D_3), fit value = 4.23] and intermediates of lipid biosynthesis, such as the carotenoid (e.g. zeaxanthin, fit value = 5.33; violaxanthin, fit value = 5.11), retinoid (e.g. retinol, fit value = 4.18), ubiquinone (e.g. 2-hexaprenylphenol, fit value = 4.34), and eicosanoid (e.g. 5-HPETE, fit value = 4.73; leukotriene B4, fit value = 4.23) biosynthetic pathways.

Discussion

Validity and Constraints of Pharmacophore Modeling. EBP, ERG2, and σ_1 are proteins that for unknown reasons form promiscuous drug receptor sites

Table 6. Gonan Hits with Fit Values >4.00 Retrieved from Search of KEGG Database (3525 metabolites) with a Modified ERG2 Pharmacophore Model (four hydrophobic, one positive ionizable, one hydrogen-bond donor)

compd	KEGG entry	chemical name	fit value
55	C11455	4,4-dimethyl-5α-cholesta-8,14,24-trien-3β-ol	5.22
56	C05111	4α-methyl-5α-cholesta-7-en-3β-ol	4.69
57	C05110	4α-methyl-5α-cholesta-8-en-3β-ol	4.64
58	C11522	4α-methyl-5α-ergosta-7,24-dien-3β-ol	4.62
34[a]	C04525	24-methylene-5α-cholest-8-en-3β-ol	4.52
33[a]	C05437	5α-cholesta-8,24-dien-3β-ol	4.48
59	C11523	4α-methyl-5α-stigmasta-7,24-dien-3β-ol	4.38
60[a]	C03845	5α-cholest-8-en-3β-ol	4.10
61	C04840	3β-hydroxy-4β-methyl-5α-cholest-7-ene-4α-carboxylate	4.08
62	C08825	4α-methyl-5α-cholest-7-en-3β-ol	4.06

[a] Actual substrates.

that bind compounds from a wide variety of chemical classes with nanomolar affinity. Their pharmacological profiles are remarkably similar. To rationalize these similarities, we built pharmacophore models for all three proteins using the chemical feature-based pharmacophore approach implemented in Catalyst. The Catalyst module HypoGen generates structure−activity relationship models from activity data—in our study K_i values of inhibitors of radioligand binding—by constructing the simplest models that best correlate the activities (estimated versus measured) of all compounds in the training set.[31] As required for successful modeling with HypoGen, the compounds in the training sets with the highest affinities were structurally diverse and the training sets covered a wide range of affinities. According to statistical analysis, our three pharmacophore models were valid, which was confirmed by their ability to well-predict the measured K_i values of the test set. The similarity of the ERG2 and σ_1 models is not surprising, given the similarity of their pharmacological profiles and the fact that HypoGen models strongly rely on conformational data sets for the compounds at the extremes of the affinity spectrum, i.e., the compounds with the highest and the lowest affinities of the training set, which are largely the same for σ_1 and ERG2. The models for σ_1 and ERG2 failed to predict the different affinities of the related compounds **8** and **24**. However, visual inspection of the compound structures revealed that unselective drugs (**11**, **13**, **22**, **23**, **25**, **32**) have long lipophilic chains attached to the basic amino group. In contrast, in σ_1-selective compounds the distance between the basic amino group and the lipophilic side chains is small (**1**, **5**, **15**, **17**), suggesting that ERG2 has stronger hydrophobic interactions than σ_1 at the lipophilic end that is farther away from the positive ionizable center. This could also explain the selectivity of **23** for ERG2 over **8**, because in **23** the distal phenyl group has a more stretched configuration than in the trans-analogue **8**. In the pharmacophore model for EBP, the same five pharmacophore features as in ERG2/σ_1 occur but have a different spatial distribution. A possible explanation for these differences would be the different reaction mechanisms of EBP and ERG2 (trans versus cis isomerization.[29] Three-dimensional structures of EBP, ERG2, and σ_1, which all are integral membrane proteins, will be required to explain the observed differences between the pharmacophore models at the molecular level.

Pharmacophore-Based Drug Discovery. All three models efficiently retrieved new compounds from drug databases, among them several chemicals that were not previously known to be ligands of EBP, σ_1, and ERG2. Except for **44**, all synthetic compounds experimentally tested had affinities <7.5 μM for all three targets (Table 5). Three and four out of the six synthetic drugs that we tested for EBP and σ_1, respectively, were even high-affinity ligands with K_i values <60 nM. Five natural steroidal alkaloids were identified as new ligands that exhibit K_i values ≤500 nM for at least one of our targets. **50** and **52** exhibited K_i values <100 nM and moderate selectivity for the σ_1 receptor, while **54** proved to be selective for ERG2 (Table 5). This remarkably high hit rate is clearly much greater than the usual hit rate of experimental high-throughput screening of complex compound libraries, which lies at or below 0.1%,[32] and it demonstrates that our pharmacophore models are well-suited to increase the efficiency of high-throughput screening by previous virtual enrichment. So far it is unknown if the interactions of widely used drugs such as **47** with EBP and σ_1 contribute to the spectrum of observed biochemical alterations (see, for example, Reid et al.[33]) or beneficial and adverse effects in patients. Since **18** caused lowering of cholesterol in patients, indicating a significant inhibition of cholesterol biosynthesis at the 3β-hydroxysteroid Δ^8-Δ^7 isomerase step,[34] experimental counterscreening of drug candidates for EBP and σ_1 was suggested.[1] With stringent search criteria (MW < 600, $K_{i\,est}$ < 100 μM) our pharmacophore models could be used as virtual filters to eliminate compounds with possible interactions with EBP or σ_1 from three-dimensional drug databases.

Affinity Prediction for the Reaction Intermediate. The ability of the ERG2 and EBP models to predict reasonable dissociation constants for the HEI of 3β-hydroxysteroid Δ^8-Δ^7 isomerization is remarkable given that the pharmacophore models were built with structurally unrelated chemicals. To our knowledge, this is the first time that enzyme affinities for a carbocationic HEI have been predicted by pharmacophore modeling. It is in line with previous suggestions that 3β-hydroxysteroid Δ^8-Δ^7 isomerization inhibitors mimick the HEI[35] and that high-affinity ligand binding to EBP occurs in the catalytic site.[1] The value obtained for ERG2 of 72 pM is in good agreement with theoretical considerations, predicting the dissociation constants of HEIs to be 10^{-11}−10^{-20} M.[36] Even though the $K_{d(HEI)}$ can be calculated from $K_{d(HEI)}/K_{m(substrate)} = k_{cat}/k_{non}$, with k_{non} being the rate of the spontanous reaction in the absence of enzyme, it is not possible to calculate k_{non} for 3β-hydroxysteroid Δ^8-Δ^7 isomerization, because acid treatment of $\Delta^{8(9)}$-sterols results solely in the formation of $\Delta^{8(14)}$-sterols.[17]

Pharmacophore-Based Retrieval of Enzyme Substrates from a Metabolite Database. The high affinity of the pharmacophore models for the HEI prompted us to investigate whether the pharmacophore models retrieved the known substrates of 3β-hydroxysteroid Δ^8-Δ^7 isomerization in a subset of the COMPOUND database of KEGG representing 3525 biochemicals of intermediary metabolism (metabolites). The rationale was to test whether pharmacophore models could not only be used to search drug databases but also to

discover unknown endogenous ligands for orphan drug receptors by virtual screening. Previously such endogenous ligands were discovered by biochemical fractionation of tissue extracts, e.g. anandamide, the endogenous cannabinoid receptor ligand,[37] or by testing candidate compounds based upon rational assumptions, e.g. bile acids, the endogenous FXR receptor regulators.[38] In these examples, however, the ligands bound with nanomolar affinity to the receptor, whereas the K_m of zymosterol for EBP is 25 μM.[1] Here we proved the concept of virtual substrate discovery by identifying the ERG2 substrates fecosterol (**34**), zymosterol (**33**), and zymostenol (**60**) among the 28 best fitting hits from a 3525 metabolite database. The higher fit values of C_4-methylated (**57**, fit value = 4.64) than for C_4-nonmethylated sterols (**60**, fit value = 4.10) suggest that the pharmacophore models for ERG2 and EBP could be further refined by introducing an excluded volume feature in the position of C_4 to better match the substrate specificity of the enzymes. So far attempts to reveal the biochemical function of σ_1 have failed. It is intriguing that, despite the similarity of the amino acid sequences, of the pharmacological profiles, and of the pharmacophores of ERG2 with σ_1, the latter has no 3β-hydroxysteroid Δ^8-Δ^7 isomerase activity.[2] The question about the true biochemical function of σ_1 and whether it is a receptor or an enzyme might be answered if endogenous compounds retrieved with a modified pharmacophore model of σ_1 were experimentally tested for both their affinities and possible biochemical transformations with recombinant σ_1.

Our results demonstrate that our five feature pharmacophore models of EBP, ERG2, and σ_1 generated with Catalyst predict reasonably well and could be not only used to enrich compound libraries prior to experimental testing but also as virtual negative filters to remove compounds for which interactions with σ_1 and EBP would not be desired. The inhibitor-based pharmacophore models predicted the expected high affinity of the unstable HEI of 3β-hydroxysteroid Δ^8-Δ^7 isomerization for EBP and ERG2, although only low-affinity steroids but not sterols were used to build these pharmacophores, confirming our previous suggestion that enzyme inhibitors bind to the catalytic site.[1,39] We suggest that inhibitor- and ligand-based pharmacophore models in combination with virtual screening of metabolite databases could be used to identify the substrates and endogenous ligands of orphan enzymes and receptors, respectively.

Experimental Section.

Radioligand Binding Assays. Binding experiments with [^{3}H]ifenprodil or (+)-[^{3}H]pentazocine were carried out as described previously[1] using recombinant proteins of σ_1 (guinea-pig 6-his-sigma$_1$-receptor,[2] GenBank accession number Z66537), ERG2 (ERG2 from *S. cerevisiae*,[40] GenBank accession number M74037), and EBP (human emopamil binding protein,[41] GenBank accession number Z37986) expressed in the ERG2 deficient strain of *S. cerevisiae* WA0 (α *his7−2 leu2−3,112 ura3−52 erg2−3*). IC_{50} values were determined from serial aqueous drug dilutions (five to seven concentrations) of a stock solution in dimethyl sulfoxide. From these values, K_i values were calculated on the basis of receptor and radioligand concentrations as described.[42] Data shown represent mean values from three or more experiments. Standard deviation (not shown) was <20%.

Molecular Modeling Studies. Computations were performed with Catalyst 4.9[43] on an Indigo O2 Workstation (255 MHz, MIPS R10000, 320 MB RAM) running Irix 6.5. Conformational models were generated with the BEST option, a maximum number of 100 conformers per compound and the default energy cutoff value of 20 kcal/mol. When compounds were tested as a mixture of stereoisomers, the regarding stereoatoms were drawn as sterically undefined. In this case, Catalyst automatically chooses the best fitting stereoisomer during model generation and fitting. HypoGen settings were left at their default values, including an uncertainty value of three. Affinity values for inactive compounds that showed K_i > 100 μM were set to 300 μM. Database searches were performed with the Fast Flexible Search method on a PC Linux cluster consisting of five nodes running Redhat Linux 9.0 with Openmosix Kernel 2.4.22 and Catalyst 4.9. The right-hand graphics in Figure 1 were created with WebLab Viewer Lite 3.5.[44]

Acknowledgment. We gratefully thank the following companies and institutions for providing sample compounds: Knoll AG, Ludwigshafen (**28**); Sanofi Synthelabo, Montpellier, France (**29**); Pfizer Central Research, US (**44**); Institute of Experimental Pharmacology, Slovak Academy of Sciences, Slovak Republic (**45**); Janssen Pharmaceutica, Belgium (**46**); Leiden/Amsterdam Center for Drug Research, The Netherlands (**48**). We thank BIOCRATES Life Sciences GmbH, Austria, for providing the subset of the KEGG database. This work was supported by grants from Fonds zur Förderung der Wissenschaftlichen Forschung (P17007 to F.F.M. and P12689 MOB to H.G.), the Dr. Legerlotz foundation (Grant 2004 to. F.F.M.), and the Jubiläumsfonds of the Austrian National Bank (P 8303 to H.G.).

Supporting Information Available: Pharmacophore model details for the three original HypoGen models. This material is available free of charge via the Internet at http://pubs.acs.org.

References

(1) Moebius, F. F.; Reiter, R. J.; Bermoser, K.; Glossmann, H.; Cho, S. Y.; Paik, Y. K. Pharmacological analysis of sterol Δ^8-Δ^7 isomerase proteins with [^{3}H]ifenprodil. *Mol. Pharmacol.* **1998**, *54*, 591−598.
(2) Hanner, M.; Moebius, F. F.; Flandorfer, A.; Knaus, H. G.; Striessnig, J.; Kempner, E.; Glossmann, H. Purification, molecular cloning, and expression of the mammalian sigma$_1$-binding site. *Proc. Natl. Acad. Sci. U.S.A.* **1996**, *93*, 8072−8077.
(3) Moebius, F. F.; Striessnig, J.; Glossmann, H. The mysteries of sigma receptors: New family members reveal a role in cholesterol synthesis. *Trends Pharmaco.l Sci.* **1997**, *18*, 67−70.
(4) Bowen, W. D. Sigma receptors: Recent advances and new clinical potentials. *Pharm. Acta Helv.* **2000**, *74*, 211−218.
(5) Moebius, F. F.; Reiter, R. J.; Hanner, M.; Glossmann, H. High affinity of sigma 1-binding sites for sterol isomerization inhibitors: Evidence for a pharmacological relationship with the yeast sterol C8−C7 isomerase. *Br. J. Pharmacol.* **1997**, *121*, 1−6.
(6) Ablordeppey, S. Y.; El-Ashmawy, M.; Fischer, J. B.; Glennon, R. A. A CoMFA investigation of sigma receptor binding affinity: Reexamination of a spurious sigma ligand. *Eur. J. Med. Chem.* **1998**, *33*, 625−633.
(7) Huang, Y.; Hammond, P. S.; Wu, L.; Mach, R. H. Synthesis and structure−activity relationships of N−(1-benzylpiperidin-4-yl)-arylacetamide analogues as potent σ_1 receptor ligands. *J. Med. Chem.* **2001**, *44*, 4404−4415.
(8) Gund, T. M.; Floyd, J.; Jung, D. Molecular modeling of σ1 receptor ligands: A model of binding conformational and electrostatic considerations. *J. Mol. Graph. Model.* **2004**, *22*, 221−230.
(9) Jung, D.; Floyd, J.; Gund, T. M. A comparative molecular field analysis (CoMFA) study using semiempirical, density functional, ab initio methods and pharmacophore derivation using DISCOtech on sigma 1 ligands. *J. Comput. Chem.* **2004**, *25*, 1385−1399.
(10) Krovat, E. M.; Langer, T. Non-Peptide Angiotensin II Receptor Antagonists: Chemical Feature Based Pharmacophore Identification. *J. Med. Chem.* **2003**, *46*, 716−726.

(11) Kanehisa, M. A database for post-genome analysis. *Trends Genet.* **1997**, *13*, 375−376.
(12) Kanehisa, M.; Goto, S. KEGG: Kyoto Encyclopedia of Genes and Genomes. *Nucleic Acids Res.* **2000**, *28*, 27−30.
(13) Moebius, F. F.; Burrows, G. G.; Striessnig, J.; Glossmann, H. Biochemical characterization of a 22-kDa high affinity antiischemic drug-binding polypeptide in the endoplasmic reticulum of guinea pig liver: Potential common target for antiischemic drug action. *Mol. Pharmacol.* **1993**, *43*, 139−148.
(14) Moebius, F. F.; Bermoser, K.; Reiter, R. J.; Hanner, M.; Glossmann, H. Yeast sterol C_8−C_7 isomerase: Identification and characterization of a high-affinity binding site for enzyme inhibitors. *Biochemistry* **1996**, *35*, 16871−16878.
(15) *Sybyl 6.91*; Tripos Inc.: St. Louis, MO, 2003.
(16) Glennon, R. A.; Ablordeppey, S. Y.; Ismaiel, A. M.; El-Ashmawy, M. B.; Fischer, J. B.; Howie, K. B. Structural features important for σ_1 receptor binding. *J. Med. Chem.* **1994**, *37*, 1214−1219.
(17) Nes, W. D.; Zhou, W.; Dennis, A. L.; Li, H.; Jia, Z.; Keith, R. A.; Piser, T. M.; Furlong, S. T. Purification, characterization and catalytic properties of human sterol 8-isomerase. *Biochem. J.* **2002**, 367, 587−599.
(18) Danso-Danquah, R.; Bai, X.; Zhang, X.; Mascarella, S. W.; Williams, W.; Sine, B.; Bowen, W. D.; Carroll, F. I. Synthesis and σ binding properties of 2′-substituted 5,9 alpha-dimethyl-6,7-benzomorphans. *J. Med. Chem.* **1995**, *38*, 2978−2985.
(19) Steindl, T.; Langer, T. Influenza Virus Neuraminidase Inhibitors: Generation and comparison of structure-based and common feature pharmacophore hypotheses and their application in virtual screening. *J. Chem. Inf. Comput. Sci.* **2004**, *44*, 1849−1856.
(20) Funk, O. F.; Kettmann, V.; Drimal, J.; Langer, T. Chemical function based pharmacophore generation of endothelin-A selective receptor antagonists. *J. Med. Chem.* **2004**, *47*, 2750−2760.
(21) Langer, T.; Krovat, E. M. Chemical feature-based pharmacophores and virtual library screening for discovery of new leads. *Curr. Opin. Drug Discov. Devel.* **2003**, *6*, 370−376.
(22) Wikstroem, H.; Andersson, B.; Elebring, T.; Svensson, K.; Carlsson, A.; Largent, B. N-Substituted 1,2,3,4,4a,5,6,10b-octahydrobenzo[*f*]quinolines and 3-phenylpiperidines: Effects on central dopamine and σ receptors. *J. Med. Chem.* **1987**, *30*, 2169−2174.
(23) Perregaard, J.; Moltzen, E. K.; Meier, E.; Sanchez, C. σ Ligands with Subnanomolar Affinity and Preference for the σ_2 Binding Site. 1. 3-(ω-Aminoalkyl)-1*H*-indoles. *J. Med. Chem.* **1995**, *38*, 1998−2008.
(24) Berardi, F.; Ferorelli, S.; Colabufo, N. A.; Leopoldo, M.; Perrone, R.; Tortorella, V. A multireceptorial binding reinvestigation on an extended class of σ ligands: N-[ω-(Indan-1-yl and tetralin-1-yl)alkyl] derivatives of 3,3-dimethylpiperidine reveal high affinities towards σ_1 and EBP sites. *Bioorg. Med. Chem.* **2001**, *9*, 1325−1335.
(25) Bowen, W. D. Sigma Receptors and Iboga Alkaloids. In *The Alkaloids*; Alper, K. R., Glick, S. D. Eds.; Academic Press: New York, 2001; Vol. 56, Chapter 9, pp 173−191.
(26) Tokuda, M.; Kawabe, N.; Hanamura, H.; Tokuda, C.; Tien, J.; Fu, X.; Ding, L. (Toray Industries, Inc., Japan; Zongoo Kuushueyuen Chendo Senu). Alkaloids for the treatment of central nervous system disorders. Jpn. Kokai Tokkyo Koho 2000−256326, 2000; *Chem Abstr. 133*, 232853.
(27) Cooper, M. K.; Porter, J. A.; Young, K. E.; Beachy, P. A. Teratogen-mediated inhibition of target tissue response to *Shh* signaling. *Science* **1998**, *280*, 1603−1607.
(28) Chen, J. K.; Taipale, J.; Cooper, M. K.; Beachy, P. A. Inhibition of Hedgehog signaling by direct binding of cyclopamine to Smoothened. *Genes Dev.* **2002**, *16*, 2743−2748.
(29) Akhtar, M.; Rahimtula, A. D.; Wilton, D. C. The stereochemistry of hydrogen elimination from C-7 in cholesterol and ergosterol biosynthesis. *Biochem. J.* **1970**, *117*, 539−542.
(30) Paik, Y. K.; Billheimer, J. T.; Magolda, R. L.; Gaylor, J. L. Microsomal enzymes of cholesterol biosynthesis from lanosterol. Solubilization and purification of steroid 8-isomerase. *J. Biol. Chem.* **1986**, *261*, 6470−6477.
(31) Kurogi, Y.; Guner, O. F. Pharmacophore modeling and three-dimensional database searching for drug design using Catalyst. *Curr. Med. Chem.* **2001**, *8*, 1035−1055.
(32) Oprea, T. I. Current trends in lead discovery: Are we looking for the appropriate properties? *J. Comput.-Aided Mol. Des.* **2002**, *16*, 325−334.
(33) Reid, I. R.; Eastell, R.; Fogelman, I.; Adachi, J. D.; Rosen, A.; Netelenbos, C.; Watts, N. B.; Seeman, E.; Ciaccia, A. V.; Draper, M. W. A comparison of the effects of raloxifene and conjugated equine estrogen on bone and lipids in healthy postmenopausal women. *Arch. Intern. Med.* **2004**, *164*, 871−879.
(34) Gylling, H.; Pyrhonen, S.; Mantyla, E.; Maenpaa, H.; Kangas, L.; Miettinen, T. A. Tamoxifen and toremifene lower serum cholesterol by inhibition of Δ8-cholesterol conversion to lathosterol in women with breast cancer. *J. Clin. Oncol.* **1995**, *13*, 2900−2905.
(35) Rahier, A.; Taton, M. Sterol biosynthesis: Strong inhibition of maize $\Delta^{5,7}$-sterol Δ^7-reductase by novel 6-aza-*B*-homosteroids and other analogues of a presumptive carbocationic intermediate of the reduction reaction. *Biochemistry* **1996**, *35*, 7069−7076.
(36) Schloss, J. V. Significance of slow-binding enzyme inhibition and its relationship to reaction-intermediate analogues. *Acc. Chem. Res.* **1988**, *21*, 348−353.
(37) Devane, W. A.; Hanus, L.; Breuer, A.; Pertwee, R. G.; Stevenson, L. A.; Griffin, G.; Gibson, D.; Mandelbaum, A.; Etinger, A.; Mechoulam, R. Isolation and structure of a brain constituent that binds to the cannabinoid receptor. *Science* **1992**, *258*, 1946−1949.
(38) Makishima, M.; Okamoto, A. Y.; Repa, J. J.; Tu, H.; Learned, R. M.; Luk, A.; Hull, M. V.; Lustig, K. D.; Mangelsdorf, D. J.; Shan, B. Identification of a nuclear receptor for bile acids. *Science* **1999**, *284*, 1362−1365.
(39) Moebius, F. F.; Soellner, K. E. M.; Fiechtner, B.; Huck, C. W.; Bonn, G.; Glossmann, H. Histidine^{77}, glutamic acid^{81}, glutamic acid^{123}, threonine^{126}, asparagine^{194}, and tryptophan^{197} of the human emopamil binding protein are required for in vivo sterol Δ8-Δ7 isomerization. *Biochemistry* **1999**, *38*, 1119−1127.
(40) Ashman, W. H.; Barbuch, R. J.; Ulbright, C. E.; Jarrett, H. W.; Bard, M. Cloning and disruption of the yeast C-8 sterol isomerase gene. *Lipids* **1991**, *26*, 628−632.
(41) Hanner, M.; Moebius, F. F.; Weber, F.; Grabner, M.; Striessnig, J.; Glossmann, H. Phenylalkylamine Ca^{2+} antagonist binding protein. Molecular cloning, tissue distribution, and heterologous expression. *J. Biol. Chem.* **1995**, *270*, 7551−7557.
(42) Linden, J. Calculating the dissociation constant of an unlabeled compound from the concentration required to displace radiolabel binding by 50%. *J. Cycl. Nucleotide Res.* **1982**, *8*, 163−172.
(43) *Catalyst 4.9*; Accelrys: San Diego, CA, 2003.
(44) *WebLab Viewer Lite 3.5*; Accelrys (formerly Molecular Simulations Inc.): San Diego, CA, 1999.

JM049073+